

## Optically actuated thermocapillary movement of gas bubbles on an absorbing substrate

Aaron T. Ohta, Arash Jamshidi, Justin K. Valley, Hsan-Yin Hsu, and Ming C. Wu<sup>a)</sup>  
*Department of Electrical Engineering and Computer Sciences, University of California, Berkeley, California 94720 and Berkeley Sensor & Actuator Center, University of California, Berkeley, California 94720*

(Received 4 May 2007; accepted 23 July 2007; published online 14 August 2007)

The authors demonstrate an optical manipulation mechanism of gas bubbles for microfluidic applications. Air bubbles in a silicone oil medium are manipulated via thermocapillary forces generated by the absorption of a laser in an amorphous silicon thin film. In contrast to previous demonstrations of optically controlled thermally driven bubble movement, transparent liquids can be used, as the thermal gradient is formed from laser absorption in the amorphous silicon substrate, and not in the liquid. A variety of bubbles with volumes ranging from 19 pl to 23 nl was transported at measured velocities of up to 1.5 mm/s. © 2007 American Institute of Physics. [DOI: 10.1063/1.2771091]

Gas bubbles in microfluidic devices can serve many functions, including acting as pumps,<sup>1</sup> valves,<sup>2</sup> mixers,<sup>3</sup> and switches,<sup>4</sup> and performing Boolean logic operations.<sup>5</sup> Typically, bubbles are carried passively by fluid flow in microfluidic channels. To achieve the active positioning of gas bubbles or liquid droplets, many different methods may be used, such as dielectrophoresis,<sup>6</sup> electrowetting,<sup>7,8</sup> optoelectrowetting,<sup>9</sup> and evaporation.<sup>10</sup> In addition, by altering surface tension, thermal gradients can be used to drive the motion of gas bubbles in liquids, or liquid droplets in air or other immiscible liquids. Surface tension is dependent on several factors, including temperature; thus, a thermal gradient creates a surface temperature gradient, which drives a fluid motion, known as thermocapillary force or the thermal Marangoni effect.<sup>11</sup> As a result, sufficient thermal gradients can drive the motion of bubbles,<sup>1,4,11</sup> droplets,<sup>12–15</sup> or thin films of fluids.<sup>16,17</sup>

Typically, thermocapillary forces are created by integrated resistive heating elements.<sup>1,4,11,13,14,16</sup> However, recent work has shown that the thermal gradients necessary to generate thermocapillary-driven bubble or droplet movement can be created by the absorption of a laser beam in a liquid.<sup>12,15,18</sup> Such optically controlled actuation has advantages over conventional dielectrophoresis, electrowetting, and resistive heating methods, as it is easier to address a large array of bubbles using optical patterns. Furthermore, optically controlled actuation is more flexible and more easily reconfigurable than resistive heating elements. However, the properties and chemistry of the liquids compatible with this method are limited by the requirement of an optically absorbing liquid.

Here, we demonstrate the trapping and transport of air bubbles, driven by an optically actuated thermocapillary force arising from the laser heating of an absorbing substrate. The use of an absorbing substrate is more flexible than using absorbing liquids, as it makes optically actuated thermocapillary forces independent of the optical properties of the liquids or gases. Furthermore, we use an inexpensive material for the absorbing substrate, allowing it to act as a disposable surface to minimize the cross contamination of sensitive

samples. Other work that relies on the heating of a substrate produces Marangoni forces via surface plasmon heating of a thin gold film on a quartz substrate.<sup>19–22</sup>

The optically induced heating of the absorbing substrate creates a thermal gradient in the substrate and the liquid media. This thermal gradient affects the surface tension of the liquid media, as most liquids have a constant, negative value of  $\partial\sigma/\partial T$ , where  $\sigma$  is the surface tension and  $T$  is the temperature. Thus, the presence of a temperature gradient will decrease the surface tension in the warmer region, creating a flow toward the colder region as the liquid attempts to minimize the total surface energy. As a result of this thermally induced liquid movement, bubbles in the liquid move toward the high-temperature regions, such as those created by optically induced heating. Once a bubble is centered above a radially symmetric thermal gradient, it is stably trapped, as the thermally induced forces balance.

In order to create optically actuated thermocapillary forces, we utilize an absorbing substrate consisting of a 0.85-mm-thick glass slide coated with a 100-nm-thick layer of indium tin oxide, followed by a 1- $\mu\text{m}$ -thick layer of hydrogenated amorphous silicon (*a*-Si:H), which absorbs light in the visible and UV wavelengths (Fig. 1). A 100- $\mu\text{m}$ -high

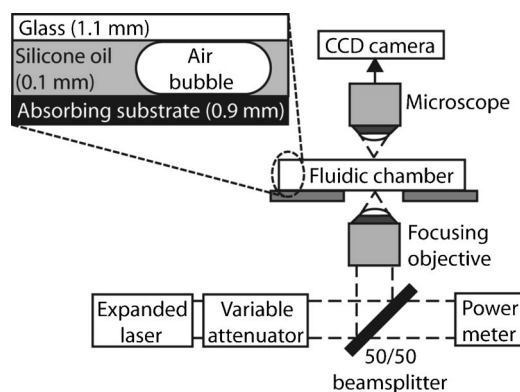


FIG. 1. Experimental setup for the optically actuated thermocapillary movement of air bubbles. A 10 mW, 635 nm laser is focused onto the absorbing substrate of a fluidic chamber by a 20 $\times$  objective lens. Air bubbles in the silicone oil have a contact angle of approximately 180 $^\circ$ , as the oil completely wets the surface of the substrate.

<sup>a)</sup>Electronic mail: wu@eecs.berkeley.edu

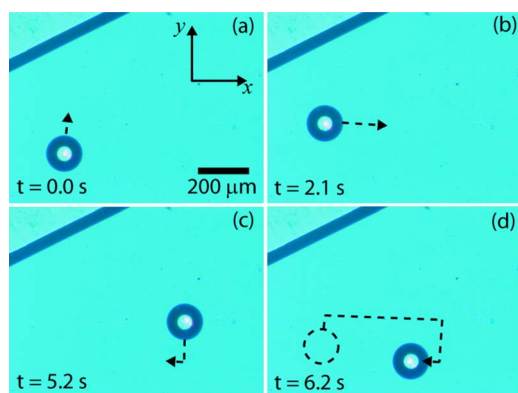


FIG. 2. (Color online) Optically actuated thermocapillary movement of an air bubble in silicone oil. A 114- $\mu\text{m}$ -diameter (1.0 nL) bubble is trapped in the thermal trap created by a laser focused on the absorbing substrate (a). The oil/air meniscus can be seen at the top left. The bubble follows the position of the laser spot, as it is scanned in the positive  $y$  direction (b) and then in the positive  $x$  direction (c). The bubble is then moved in the negative  $y$  and negative  $x$  directions (d). The initial bubble position is indicated by a dashed circle, and the approximate trajectory of the bubble is indicated by a dashed line.

fluidic chamber was formed between the absorbing substrate and a 1.1-mm-thick glass slide and filled with approximately 20  $\mu\text{l}$  of silicone oil (Dow Corning 200 $\text{\textcircled{R}}$  fluid). Air bubbles are trapped during the loading of the fluidic chamber, with volumes ranging from approximately 85 pl to 23 nL. Contact angle measurements at the oil/air/substrate interface show that the silicone oil completely wets the  $a\text{-Si:H}$  surface. The laser source that provides the optically induced heating is a 10 mW, 635 nm semiconductor laser. At this wavelength, it was empirically determined that the  $a\text{-Si:H}$ -coated substrate absorbs 94% of the incident light, not accounting for reflections at the air/substrate and substrate/liquid interfaces. The output of the semiconductor laser is expanded to fill the aperture of a 20 $\times$  microscope objective, which focuses the beam to a 6- $\mu\text{m}$ -diameter spot on the surface of the absorbing substrate. The laser intensity is controlled with a variable attenuator, and the laser power is monitored using an optical power meter (Hewlett-Packard 8153A).

The optically actuated thermocapillary movement of a 114- $\mu\text{m}$ -diameter air bubble in silicone oil is shown in Fig. 2. The air bubble is initially positioned directly over the area illuminated by the laser [Fig. 2(a)]. The laser illumination position is subsequently scanned across the substrate by manually adjusting the position of the focusing objective relative to the fluidic chamber. From the original location, the laser spot is translated in the positive  $y$  direction [Fig. 2(b)], then in the positive  $x$  direction [Fig. 2(c)], and then in the negative  $y$  and negative  $x$  directions [Fig. 2(d)]. The dashed circle in Fig. 2(d) indicates the initial position of the bubble, and the dashed line indicates the approximate trajectory. The silicone oil/air meniscus is visible in the upper-left corner of each image as a reference. The image sequence in Fig. 2 spans 6.2 s, during which the bubble attains velocities of approximately 800  $\mu\text{m/s}$ .

We have been able to reproducibly transport air bubbles with diameters ranging from 33 to 329  $\mu\text{m}$ , which correspond to a volume range of 19 pl–23 nL. (A spherical volume is assumed for bubbles with diameters smaller than the chamber height of 100  $\mu\text{m}$ ; for larger bubbles, the cylindrical volume formula is used.) The maximum velocity at which these bubbles can be transported is linearly dependent

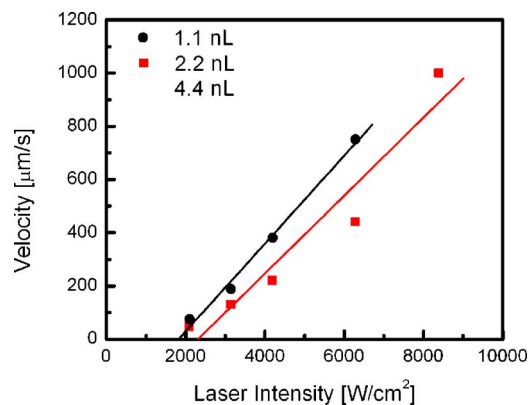


FIG. 3. (Color online) Optically actuated thermocapillary movement-induced velocities of air bubbles as a function of laser intensity. The solid lines are linear fits to the data points.

on the intensity of the laser source (Fig. 3). This is expected, as the laser intensity is directly proportional to induced thermal gradient produced by the optical absorption. The measured velocities are the maximum translation rates of the bubbles across the surface of the absorbing substrate, as the optical pattern is fixed and the substrate is moved by a motorized stage. The maximum translation rate of the motorized stage is 1 mm/s, limiting the maximum velocity that can be measured with this method. Bubbles with diameters of approximately 100  $\mu\text{m}$  or less (volumes of 0.5 nL or less) easily exceed maximum velocity of 1 mm/s, especially at the higher laser intensities. However, analysis of video captured during the bubble transport allows us to approximate the maximum velocity of bubbles less than 0.5 nL in volume to be approximately 1.5 mm/s at the lowest measured light intensity, 2  $\text{kW/cm}^2$ .

The optically induced temperature gradient can be determined using the temperature-dependent surface tension equation,  $\text{grad}(\sigma) = (\partial\sigma/\partial T)\text{grad}(T)$ , and the Navier-Stokes equation. The calculated temperature gradient required to move a bubble at 1.5 mm/s is approximately 4000  $\text{K m}^{-1}$ , given the viscosity of the silicone oil,<sup>23</sup>  $\mu = 4.56 \times 10^{-3}$  Pa s, and the temperature coefficient of the surface tension,<sup>23</sup>  $\gamma_T = -\partial\sigma/\partial T = 7.2 \times 10^{-5}$   $\text{N m}^{-1} \text{K}^{-1}$ . In the geometry of the optically actuated thermocapillary device, this corresponds to a temperature rise of approximately 0.5  $^\circ\text{C}$  at the oil/ $a\text{-Si:H}$  interface. This value was verified experimentally using a 50- $\mu\text{m}$ -thick thermocouple (Omega Engineering, type T; resolution=0.1  $^\circ\text{C}$ ) affixed to the  $a\text{-Si:H}$  substrate. The temperature measurements were taken with the fluidic system on an aluminum microscope stage, surrounded by a room temperature environment.

Further possibilities of optically actuated thermocapillary movement include the usage of spatial light modulators to simultaneously create multiple bubble traps, a technique that has widespread usage in the optical trapping community.<sup>24,25</sup> In addition, this technique is not limited to excitation by a coherent source; incoherent sources can be used, as long as a sufficient thermal gradient is generated. Furthermore, the absorbing substrate used in these experiments has not been optimized for the generation of a thermal gradient, as it was originally designed for use as an electrode for an optoelectronic tweezer device.<sup>25</sup> Thus, improvements may be made to the absorbing substrate to create higher thermal gradients. This may include alternate materials that have

suitable optical absorption coefficients and low thermal conductivities.

Optically actuated thermocapillary bubble movement on an absorbing substrate enables the actuation of bubbles in a variety of liquids, independent of the optical properties of the liquid. This capability can be used in microfluidic applications as a way to optically control fluid pumping or switching.<sup>5</sup> The optical addressing of this technique is also amenable to the creation of dense arrays of optically controlled bubbles.

Funding is provided by the Institute for Cell Mimetic Space Exploration (CMISE), a NASA University Research, Engineering, and Technology Institute (URETI), and by the National Institutes of Health through the NIH Roadmap for Medical Research, Grant No. PN2 EY018228. One of the authors (A.T.O.) is supported by a National Science Foundation Graduate Research fellowship.

<sup>1</sup>T. K. Jun and C. J. Kim, *J. Appl. Phys.* **83**, 5658 (1998).

<sup>2</sup>S. Z. Hua, F. Sachs, D. X. Yang, and H. D. Chopra, *Anal. Chem.* **74**, 6392 (2002).

<sup>3</sup>P. Garstecki, M. J. Fuerstman, M. A. Fischbach, S. K. Sia, and G. M. Whitesides, *Lab Chip* **6**, 207 (2006).

<sup>4</sup>T. Sakata, H. Togo, M. Makihara, F. Shimokawa, and K. Kaneko, *J. Light-wave Technol.* **19**, 1023 (2001).

<sup>5</sup>M. Prakash and N. Gershenfeld, *Science* **315**, 832 (2007).

<sup>6</sup>J. A. Schwartz, J. V. Vykoukal, and P. R. C. Gascoyne, *Lab Chip* **4**, 11 (2004).

<sup>7</sup>J. Lee and C. J. Kim, *J. Microelectromech. Syst.* **9**, 171 (2000).

<sup>8</sup>M. G. Pollack, A. D. Shenderov, and R. B. Fair, *Lab Chip* **2**, 96 (2002).

<sup>9</sup>P. Y. Chiou, H. Moon, H. Toshiyoshi, C. J. Kim, and M. C. Wu, *Sens. Actuators, A* **104**, 222 (2003).

<sup>10</sup>G. L. Liu, J. Kim, Y. Lu, and L. P. Lee, *Nat. Mater.* **5**, 27 (2006).

<sup>11</sup>N. O. Young, J. S. Goldstein, and M. J. Block, *J. Fluid Mech.* **6**, 350 (1959).

<sup>12</sup>K. T. Kotz, K. A. Noble, and G. W. Faris, *Appl. Phys. Lett.* **85**, 2658 (2004).

<sup>13</sup>R. H. Farahi, A. Passian, T. L. Ferrell, and T. Thundat, *Appl. Phys. Lett.* **85**, 4237 (2004).

<sup>14</sup>A. A. Darhuber, J. P. Valentino, J. M. Davis, S. M. Troian, and S. Wagner, *Appl. Phys. Lett.* **82**, 657 (2003).

<sup>15</sup>B. A. Bezuglyi and N. A. Ivanova, *Fluid Dyn.* **41**, 278 (2006).

<sup>16</sup>D. E. Kataoka and S. M. Troian, *Nature (London)* **402**, 794 (1999).

<sup>17</sup>N. Garnier, R. O. Grigoriev, and M. F. Schatz, *Phys. Rev. Lett.* **91**, 054501 (2003).

<sup>18</sup>N. A. Ivanova and B. A. Bezuglyi, *Tech. Phys. Lett.* **32**, 854 (2006).

<sup>19</sup>R. H. Farahi, A. Passian, T. L. Ferrell, and T. Thundat, *Opt. Lett.* **30**, 616 (2005).

<sup>20</sup>R. H. Farahi, A. Passian, S. Zahrai, A. L. Lereu, T. L. Ferrell, and T. Thundat, *Ultramicroscopy* **106**, 815 (2006).

<sup>21</sup>A. L. Lereu, A. Passian, R. H. Farahi, S. Zahrai, and T. Thundat, *Journal of the European Optical Society—Rapid Publications* **1**, 06030 (2006).

<sup>22</sup>A. Passian, S. Zahrai, A. L. Lereu, R. H. Farahi, T. L. Ferrell, and T. Thundat, *Phys. Rev. E* **73**, 066311 (2006).

<sup>23</sup>E. Lajeunesse and G. M. Homsy, *Phys. Fluids* **15**, 308 (2003).

<sup>24</sup>D. G. Grier, *Nature (London)* **424**, 810 (2003).

<sup>25</sup>P. Y. Chiou, A. T. Ohta, and M. C. Wu, *Nature (London)* **436**, 370 (2005).